coatings

Supplementary Materials Rare Biogeochemical Phenomenon Associated to Manganese Patinas on Mural Painting and Granite Ashlars

Bruno Campos [1,2], Alexandra Marco [1,2], David M. Freire-Lista [3,4], Nuno Durães [5], Joaquin Silvestre-Albero [6], Eduardo Ferreira da Silva [5], Eduarda Vieira [1], Manuela Pintado [2] and Patrícia R. Moreira [1,2,*]

[1] CITAR Research Centre for Science and Technology of the Arts, Portuguese Catholic University, R. de Diogo Botelho,1327, 4169-005 Porto, Portugal; bcampos@porto.ucp.pt (B.C.); alexandra.marco.ma@gmail.com (A.M.); evieira@porto.ucp.pt (E.V.)
[2] CBQF Centre for Biotechnology and Fine Chemistry, Portuguese Catholic University, R. de Diogo Botelho,1327, 4169-005 Porto, Portugal; mpintado@porto.ucp.pt
[3] Department of Geology, UTAD Universidade de Trás-os-Montes e Alto Douro. Quinta de Prados, 5001-801 Vila Real, Portugal; davidfreire@utad.pt
[4] CGeo Centro de Geociências da Universidade de Coimbra, Universidade de Coimbra—Polo II, Rua Silvino Lima, 3030-790 Coimbra, Portugal;
[5] GEOBIOTEC Research Centre, Department of Geosciences, University of Aveiro, Campus Universitário de Santiago, 3810-193 Aveiro, Portugal; nunoduraes@ua.pt (N.D.); eafsilva@ua.pt (E.F.d.S.)
[6] Departamento de Química Inorgánica, UA Universidad de Alicante, Carretera de San Vicente del Raspeig s/n, 03690 San Vicente del Raspeig, Spain; joaquin.silvestre@ua.es
* Correspondence: prmoreira@ucp.pt

Citation: Campos, B.; Marco, A.; Freire-Lista, D.M.; Durães, N.; Silvestre-Albero, J.; da Silva, E.; Vieira, E.; Pintado, M.; Moreira, P.R. Rare Biogeochemical Phenomenon Associated to Manganese Patinas on Mural Painting and Granite Ashlars. *Coatings* **2021**, *11*, 917. https://doi.org/10.3390/coatings11080917

Academic Editor: Maurizio Licchelli

Received: 21 June 2021
Accepted: 27 July 2021
Published: 30 July 2021

Materials and Methods

Case study

The foundation of Sta. Marinha church dates from the 12th century and the architecture is markedly influenced by a Romanesque style, made of granite ashlars (Figure S5a). The church inner walls are partially decorated with *frescoes* on the chancel and on the nave, showing two campaigns, dating from 15th and 16th centuries, being the latter attributed to the painter Arnaus. The 15th century mortar has been designated as M1 and the 16th century as M2. The north wall of the nave is covered with two pictorial campaigns composed by three registers, (i) a superior register showing a tinny fragment of a *grotteschi* frame with black background; (ii) a middle register representing the Passion of Christ identified by the Christ on the Mount of Olives and the Kiss of Judas; and (iii) an inferior register showing a representation of three saints—S. Antão, S. Brás and S. Roque (Figure S5b) [1]. The black-blue patina problem is observed in the inferior register at 1.70 m from the ground, confined to an area of 0.18 m^2 (0.3 m × 0.6 m) (Figure S5b). The report of black-blue coloration on *frescoes* do not have a specific date since its very beginning but local citizens claim that it has been growing until the size and extent of the actual patina.

Figures

Figure S1. Sampling sites for ICP-MS analysis.

(**a**) (**b**)

Figure S2. In situ sampling sites of granite stains from (**a**) front wall and (**b**) back wall of mural painting.

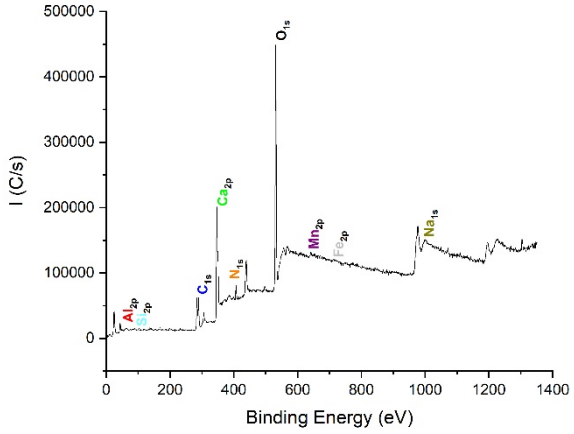
I (C/s)
Binding Energy (eV)
O1s
Ca2p
C1s
N1s
Mn2p
Na1s
Al2p
Si2p

(**a**)

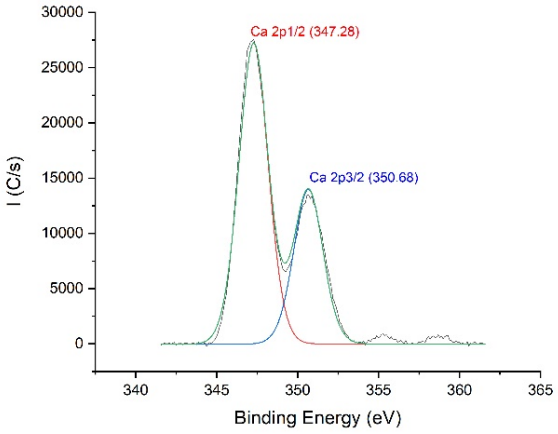
I (C/s)
Binding Energy (eV)
Ca 2p1/2 (347.28)
Ca 2p3/2 (350.68)

(**b**)

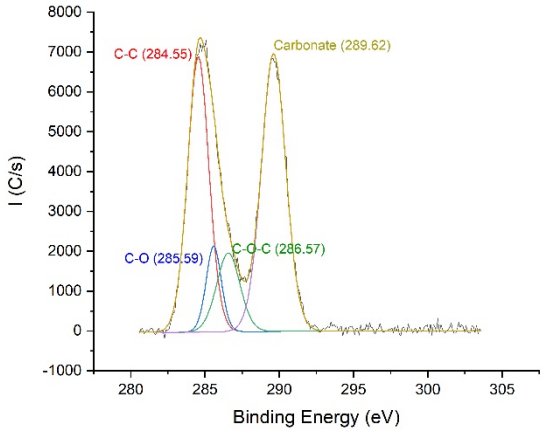
I (C/s)
Binding Energy (eV)
C-C (284.55)
Carbonate (289.62)
C-O (285.59)
C-O-C (286.57)

(**c**)

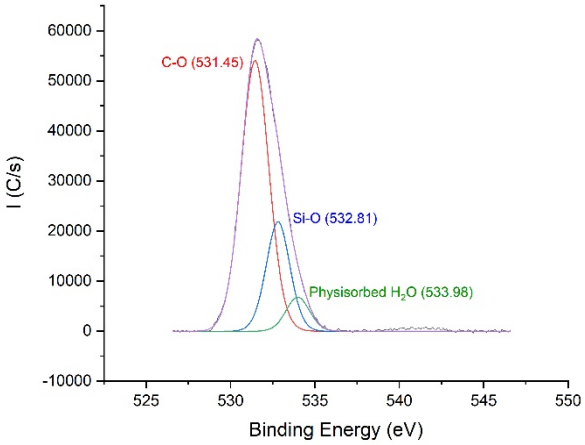
I (C/s)
Binding Energy (eV)
C-O (531.45)
Si-O (532.81)
Physisorbed H2O (533.98)

(**d**)

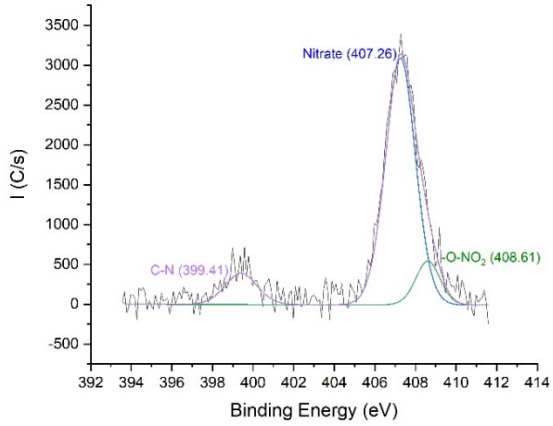
I (C/s)
Binding Energy (eV)
Nitrate (407.26)
C-N (399.41)
O-NO2 (408.61)

(**e**)

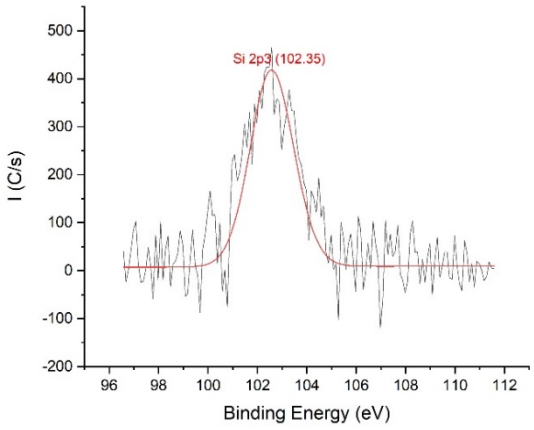
I (C/s)
Binding Energy (eV)
Si 2p3 (102.35)

(**f**)

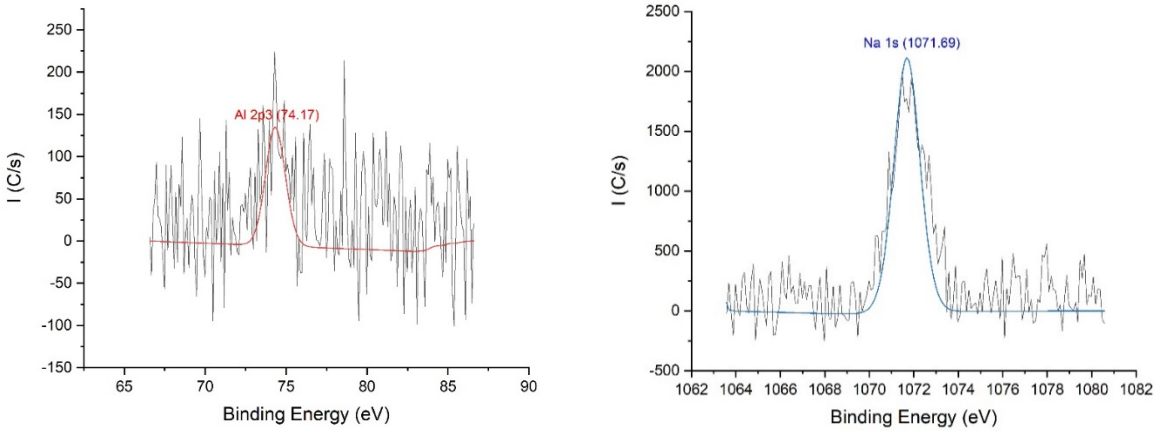

(**g**) (**h**)

Figure S3. (**a**) XPS survey spectra of MP3; high resolution spectra of (**b**) Ca 2*p* (**c**). C 1*s*. (**d**) O 1*s*. (**e**) N 1*s*. (**f**) Si 2*p*3. (**g**) Al 2*p*3 and (**h**) Na 1*s*.

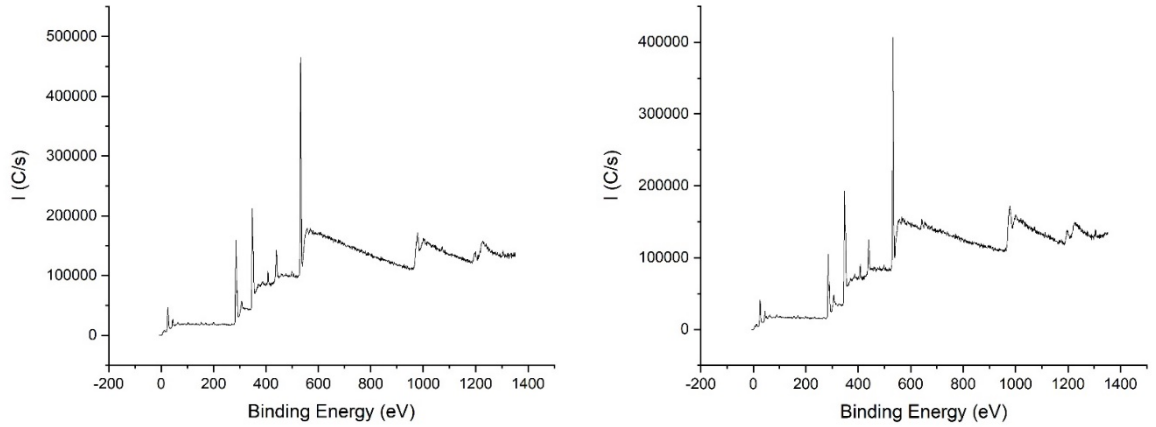

(**a**) (**b**)

Figure S4. XPS survey spectra of (**a**) MP1 and (**b**) MP2.

(**a**) (**b**)

Figure S5. (**a**) Exterior façade of Sta. Marinha Church, Vila Marim, Portugal; (**b**) North wall decorated with mural painting.

Tables

Table S1. Description of samples collected from Sta. Marinha Church and submitted to chemical analysis.

Ref.	Description
GR1	Granite
GR2	Granite
X1	Phyllite
X2	Phyllite
J1	Joint between granite blocks
J2	Joint between granite blocks
Arg1	Mortar
Arg2	Mortar
G2	Granite showing black-blue patina
G3	Granite showing black-blue patina
MP1	Mural painting showing black-blue patina
MP4	Mural painting showing black-blue patina
MP6	Mural painting showing black-blue patina

Table S2. Raman assignments of pigments used in the first and second campaign.

Color	First Campaign	Second Campaign
	Wavenumber (cm^{-1})	Wavenumber (cm^{-1})
Orange	224, 295, 355 and 410 (Fe_2O_3)	232, 289, 406, 604 and 1301 (Fe_2O_3); 1054 ($PbCO_3$)
Red	253, 283 and 346 (HgS)	231, 286 and 405 (Fe_2O_3); 1088 ($CaCO_3$)
White	1088 ($CaCO_3$); 1055 ($PbCO_3$)	1088 ($CaCO_3$); 1051 ($PbCO_3$)
Black	1331 and 1613 (Carbon black)	1328 and 1591 (Carbon black)
Grey	-	1092 ($CaCO_3$); 1330,1586 and 1619 (Carbon black)

Table S3. Iron and manganese percentage of black-blue patina on granite. G0 = raw granite (without stain); Avg = average.

Sample	Fe (wt.%)	Fe_{Gn+1}/Fe_{G0}	Mn (wt.%)	Mn_{Gn+1}/Mn_{G0}	Mn/Fe
G0	1.01	-	0.08	-	-
G1	0.69	0.69	1.39	17.42	2.01
G2	0.45	0.45	1.98	24.76	4.39
G3	0.68	0.67	2.92	36.45	4.30
G4	1.08	1.07	2.20	27.46	2.03
Avg	0.73 ± 0.26	0.72 ± 0.26	2.12 ± 0.63	26.52 ± 7.86	3.18 ± 1.34

Table S4. Weight percentage of the elements present in black-blue patinas by pXRF (normalized values). Bal = stands for balance, it represents the light elements within the sample not excited by the analyser; only values above 0.10% are presented in this table.

Elements	MP1	MP2	MP3	MP4	MP5	MP6
Bal	59.39	66.61	66.08	61.18	58.81	58.52
Pb	-	-	0.31	0.13	0.11	-
Fe	1.95	0.91	1.71	0.74	0.97	0.72
Mn	1.92	1.03	2.01	1.81	1.86	1.65
V	-	0.12	-	-	-	-
Ti	0.13	0.15	-	0.13	-	-
Ca	22.37	20.00	24.79	27.25	32.05	31.86
K	0.91	1.17	0.59	0.77	0.45	0.56
Al	2.32	1.46	0.76	1.23	1.09	0.90
Si	8.19	7.52	2.79	5.43	3.02	3.14
Cl	0.60	0.56	0.43	0.44	0.45	0.41
S	1.97	0.36	0.26	0.56	0.96	1.94

Table S5. Assignments attributed to XPS peaks for MP1 and MP2 samples.

Name	MP1			MP2		
	Peak BE	Assignments	Atomic %	Peak BE	Assignments	Atomic %
C1s Scan A	284.55	Adventitious carbon	21.45	284.62	Adventitious carbon	17.05
C1s Scan B	285.89	C–O	10.83	286.14	C–O–C	7.2
C1s Scan C	288.08	O–C=O	3.63	288.21	O–C=O	3.85
C1s Scan D	289.69	Carbonate	8.00	289.83	Carbonate	8.64
N1s Scan A	400.09	C–N	0.22	399.82	C–N	0.37
N1s Scan B	407.32	Nitrate	1.53	407.24	Nitrate	2.05
N1s Scan C	408.73	–O–NO_2	1.01	408.62	–O–NO_2	0.43
O1s Scan A	531.32	C–O	16.5	531.43	C–O	23.76
O1s Scan B	532.56	Si–O	18.98	532.84	Si–O	15.72
O1s Scan C	534.04	Physisorbed H_2O	4.82	534.43	Physisorbed H_2O	6.77
Al2p3 Scan A	73.87	Al_2O_3	0.25	-	-	-
Si2p3 Scan A	102.41	SiO_2	0.93	102.73	SiO_2	0.67
Ca2p3 Scan A	347.35	$CaCO_3$	11.19	347.35	$CaCO_3$	12.24
Mn2p3 Scan A	641.39	Mn_3O_4	0.1	642.08	Mn_3O_4	0.43
Mn2p3 Scan B	643.32	MnO_2	0.06	644.56	MnO_2	0.21
Fe2p3 Scan A	710.43	Fe_3O_4	0.05	710.92	Fe_3O_4	0.12
Fe2p3 Scan B	712.9	Fe_2O_3	0.03	713.58	Fe_2O_3	0.08
Na1s Scan A	1071.86	NaCl	0.39	1071.81	NaCl	0.4

Table S6. Concentrations of major and trace elements in groundwater of Vila Marim.

Element	Unit	Groundwater
Ca	mg·L^{-1}	7.72
K		12.3
Mg		3.11
Na		11.0
Al	μg·L^{-1}	6.56
As		9.48
Ba		45.4
Co		<dl
Cr		0.13
Cu		0.91
Fe		1.78
Mn		2.12
Ni		0.48
P		566
Pb		<dl
Sr		45.2
U		0.17
Zn		3.61

dl—detection limit.

Table S7. Concentrations of major and trace elements of granite and *frescoes* affected by black-blue patina.

Element	Unit	G2	G3	MP1	MP4	MP6
Al	mg·kg^{-1}	12364	45487	10987	13970	4568
As		8.59	6.42	9.913	11.009	15.196
Ba		163	110	348	369	257
Ca		4886	8851	235,050	278,570	329,349
K		6753	30,912	5264	6092	4152
Co		86.79	48.84	13.46	12.25	16.12
Cr		16.66	24.24	14.84	20.07	17.49
Cu		10.13	16.29	44.90	247.58	237.34
Fe		15,937	68,504	9790	11,850	4946
Mg		3134	11,496	4398	3929	3177
Mn		5810	5639	4760	9207	23672
Na		457	869	3916	3743	2828
Ni		15.71	17.18	65.71	30.54	13.92
P		637	1364	541	1100	363
Pb		25.9	42.2	143.7	522.0	11336.2
Sr		27.7	33.0	713.3	710.6	519.2
U		4.51	8.14	2.84	3.41	4.56
Zn		247.83	521.05	85.15	192.95	116.96

Table S8. Similar Mn patinas found on built heritage and caves.

Mn Coatings	Place of Coating	Type of Stone/Rock	Thickness of Coating	Maximum Mn Concentration (Technique)	Mn Source	Suggested Coating Formation
Freiburger Münster—Germany [2]	External wall	Sandstone	*N.F.	7.71 wt.% (fs LA-ICP-MS)	Atmospheric dust	Leaching and redeposition of aerosol Mn followed by autocatalytic oxidation
Smithsonian Institution Building—USA [3]	External wall	Red Seneca Sandstone	200–300 μm	2.71 wt.% (X-ray microanalysis)	Atmospheric dust	Leaching and redeposition of aerosol Mn followed by autocatalytic oxidation
Neang Khmau temple—Cambodia [4]	External and Internal wall	Laterite	300–1000 μm	48 at.% (EDX)	Lateritic rock	Efflorescence and precipitation of Mn favoured by Mn-oxidizing microbes
Lauscaux Cave—France [5]	Wall and ceiling	Sandstone	*N.F.	*N.F.	Sandstone (clayey sediment)	Biogenic oxidation of Mn (by A. nepalense, a Mn oxide-depositing fungus)
Paranhos tunnel Portugal [6]	Wall and ceiling	Granite	1–100 mm	1.19 wt.% (ICP-MS)	Mn leached from soil and rocks	Biogenic oxidation of Mn
Pautler Cave—USA [7]	Wall, ceiling and floor	Limestone	*N.F.	45.4 wt.% (ICP-OES)	Mn-rich groundwater and stream water	Secondary abiotic reactions between Mn(II) and biogenic Mn(IV)

*N.F.—Not Found.

Reference

1. de Ferri, G.; Mazzini, L.; Vallotto, F.; Pojana, D. In situ non-invasive characterization of pigments and alteration products on the masonry altar of S. Maria ad Undas (Idro, Italy). *Archaeol. Anthropol. Sci.* **2019**, *11*, 609–625
2. Macholdt, D.S.; Herrmann, S.; Jochum, K.P.; Kilcoyne, A.D.; Laubscher, T.; Pfisterer, J.H.; Pöhlker, C.; Schwager, B.; Weber, B.; Weigand, M.; et al. Black manganese-rich crusts on a Gothic cathedral. *Atmos. Environ.* **2017**, *171*, 205–220, doi: 10.1016/j.atmosenv.2017.10.022.
3. Vicenzi, Z.; Grissom, E.; Livingston, C.; Weldon-Yochim, R.; Rock varnish on architectural stone: microscopy and analysis of nanoscale manganese oxide deposits on the Smithsonian Castle, Washington, DC. *Herit. Sci.* **2016**, *4*, 26, doi: 10.1186/s40494-016-0093-2.
4. Dakal, T.; Cameotra, S. Microbially induced deterioration of architectural heritages: routes and mechanisms involved. *Environ. Sci. Eur.* **2012**, *24*, 36, doi: 10.1186/2190-4715-24-36.
5. Saiz-Jimenez, C.M.; Miller, A.; Martin-Sanchez; Hernandez-Marine, P. Uncovering the origin of the black stains in Lascaux Cave in France. *Environ. Microbiol.* **2012**, *14*, 3220–3231, doi: 10.1111/1462-2920.12008.
6. Miller, A.Z.; Dionísio, A.; Braga, M.S.; Hernández-Mariné; M.; Afonso, M.J.; Muralha, V.S.F.; Herrera, L.K.; Raabe, J.; Fernandez-Cortes, A.; Cuezva, S.; Hermosin, B.; et al. Biogenic Mn oxide minerals coating in a subsurface granite environment. *Chem. Geol.* **2012**, *322–323*, 181–191, doi: 10.1016/j.chemgeo.2012.07.005.
7. Frierdich, A.J.; Hasenmueller, E.A.; Catalano, J.G. Composition and structure of nanocrystalline Fe and Mn oxide cave deposits: Implications for trace element mobility in karst systems, *Chem. Geol.* **2011**, *284*, 82–96, doi: 10.1016/j.chemgeo.2011.02.009.